

# Breaking the imaging symmetry in negative refraction lenses

Changbao Ma and Zhaowei Liu\*

Department of Electrical and Computer Engineering, University of California, San Diego, La Jolla, California  
92093-0407, USA

\*zhaowei@ece.ucsd.edu

**Abstract:** Optical lenses are pervasive in various areas of sciences and technologies. It is well known that conventional lenses have symmetrical imaging properties along forward and backward directions. In this letter, we show that hyperbolic plasmonic metamaterial based negative refraction lenses perform as either converging lenses or diverging lenses depending on the illumination directions. New imaging equations and properties that are different from those of all the existing optical lenses are also presented. These new imaging properties, including symmetry breaking as well as the super resolving power, significantly expand the horizon of imaging optics and optical system design.

© 2012 Optical Society of America

**OCIS codes:** (160.3918) Metamaterials; (220.3630) Lenses; (110.2990) Image formation theory; (350.4238) Nanophotonics and photonic crystals.

---

## References and links

1. J. Kepler, *Dioptrice* (Augsburg: Franci, 1611).
2. E. Hecht, *Optics*, 4<sup>th</sup> ed. (Addison-Wesley, 2002).
3. E. Abbe, "Beitrage zur Theorie des Mikroskops und der mikroskopischen Wahrnehmung," *Arch. Mikrosk. Anat. Entwicklungsmech.* **9**(1), 413–418 (1873).
4. Q. Wu, G. D. Feke, R. D. Grober, and L. P. Ghislain, "Realization of numerical aperture 2.0 using a gallium phosphide solid immersion lens," *Appl. Phys. Lett.* **75**(26), 4064–4066 (1999).
5. S. B. Ippolito, B. B. Goldberg, and M. S. Unlu, "High spatial resolution subsurface microscopy," *Appl. Phys. Lett.* **78**(26), 4071–4073 (2001).
6. D. R. Smith, J. B. Pendry, and M. C. K. Wiltshire, "Metamaterials and negative refractive index," *Science* **305**(5685), 788–792 (2004).
7. J. Yao, Z. Liu, Y. Liu, Y. Wang, C. Sun, G. Bartal, A. M. Stacy, and X. Zhang, "Optical negative refraction in bulk metamaterials of nanowires," *Science* **321**(5891), 930 (2008).
8. V. M. Shalaev, "Optical negative-index metamaterials," *Nat. Photonics* **1**(1), 41–48 (2007).
9. J. B. Pendry, "Negative refraction makes a perfect lens," *Phys. Rev. Lett.* **85**(18), 3966–3969 (2000).
10. N. Fang, H. Lee, C. Sun, and X. Zhang, "Sub-diffraction-limited optical imaging with a silver superlens," *Science* **308**(5721), 534–537 (2005).
11. Z. Liu, S. Durant, H. Lee, Y. Pikus, N. Fang, Y. Xiong, C. Sun, and X. Zhang, "Far-field optical superlens," *Nano Lett.* **7**(2), 403–408 (2007).
12. E. E. Narimanov, "Far-field superlens: optical nanoscope," *Nat. Photonics* **1**(5), 260–261 (2007).
13. Z. Jacob, L. V. Alekseyev, and E. Narimanov, "Optical Hyperlens: Far-field imaging beyond the diffraction limit," *Opt. Express* **14**(18), 8247–8256 (2006).
14. Z. Liu, H. Lee, Y. Xiong, C. Sun, and X. Zhang, "Far-field optical hyperlens magnifying sub-diffraction-limited objects," *Science* **315**(5819), 1686 (2007).
15. Y. Xiong, Z. Liu, and X. Zhang, "A simple design of flat hyperlens for lithography and imaging with half-pitch resolution down to 20 nm," *Appl. Phys. Lett.* **94**(20), 203108 (2009).
16. I. I. Smolyaninov, Y. J. Hung, and C. C. Davis, "Magnifying superlens in the visible frequency range," *Science* **315**(5819), 1699–1701 (2007).
17. S. Vedantam, H. Lee, J. Tang, J. Conway, M. Staffaroni, and E. Yablonovitch, "A plasmonic dimple lens for nanoscale focusing of light," *Nano Lett.* **9**(10), 3447–3452 (2009).
18. F. M. Huang and N. I. Zheludev, "Super-resolution without evanescent waves," *Nano Lett.* **9**(3), 1249–1254 (2009).
19. L. Verslegers, P. B. Catrysse, Z. Yu, and S. Fan, "Deep-subwavelength focusing and steering of light in an aperiodic metallic waveguide array," *Phys. Rev. Lett.* **103**(3), 033902–033904 (2009).
20. X. Zhang and Z. Liu, "Superlenses to overcome the diffraction limit," *Nat. Mater.* **7**(6), 435–441 (2008).

21. C. Ma, R. Agualdo, and Z. Liu, "Advances in the hyperlens," *Chin. Sci. Bull.* **55**(24), 2618–2624 (2010).
22. C. Ma and Z. Liu, "Focusing light into deep subwavelength using metamaterial immersion lenses," *Opt. Express* **18**(5), 4838–4844 (2010).
23. C. Ma and Z. Liu, "A super resolution metalens with phase compensation mechanism," *Appl. Phys. Lett.* **96**(18), 183103 (2010).
24. C. Ma and Z. Liu, "Designing super-resolution metalenses by the combination of metamaterials and nanoscale plasmonic waveguide couplers," *J. Nanophotonics* **5**(1), 051604 (2011).
25. S. Thongrattanasiri and V. A. Podolskiy, "Hypergratings: nanophotonics in planar anisotropic metamaterials," *Opt. Lett.* **34**(7), 890–892 (2009).
26. T. Zentgraf, J. Valentine, N. Tapia, J. Li, and X. Zhang, "An optical "Janus" device for integrated photonics," *Adv. Mater. (Deerfield Beach Fla.)* **22**(23), 2561–2564 (2010).
27. J. B. Pendry, D. Schurig, and D. R. Smith, "Controlling electromagnetic fields," *Science* **312**(5781), 1780–1782 (2006).
28. U. Leonhardt, "Optical conformal mapping," *Science* **312**(5781), 1777–1780 (2006).
29. C. Ma, M. A. Escobar, and Z. Liu, "Extraordinary light focusing and Fourier transform properties of gradient-index metalenses," *Phys. Rev. B* **84**(19), 195142 (2011).

## 1. Introduction

Lenses are the most fundamental and widely used elements in optics. The configuration of a lens is determined by the type of wavefront conversion to perform; basic conversions include transformation among diverging waves, converging waves and plane waves. As an object can be considered as an accumulation of point sources, a lens that converts a diverging wave to a converging one is capable to form an image of the object.

Imaging is one of the most basic functions of a lens, of which the imaging properties have been well established since the first elaboration by Kepler in 1611 [1]. As is illustrated in Fig. 1 and summarized in Table 1 [2], the image shows various characteristics when an object is placed at different locations with respect to the focal length  $f$  of a lens. Such imaging rules, which are governed by the imaging Eq. (1)  $1/s_0 + 1/s_i = 1/f$  with  $s_0$  and  $s_i$  being the object and image distances, respectively, are the foundations for ray optics and optical system design.

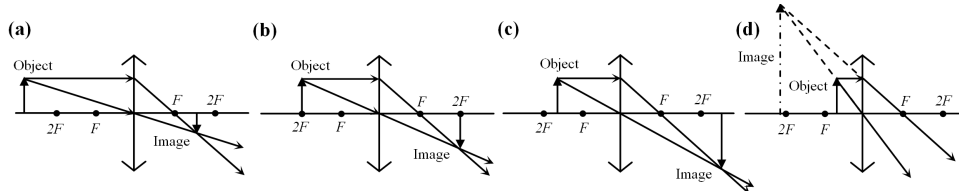


Fig. 1. Imaging behaviors of a conventional converging lens. An object is placed beyond  $2f$  in (a), at  $2f$  in (b), between  $f$  and  $2f$  in (c), and within  $f$  in (d).  $f$  is the focal length of the lens.

**Table 1. Imaging Properties of a Conventional Converging Lens**

Object		Image		
Location	Type	Location	Orientation	Relative size
$\infty > s > 2f$	Real	$f < p < 2f$	Inverted	Minified
$s = 2f$	Real	$p = 2f$	Inverted	Same size
$f < s < 2f$	Real	$2f < p < \infty$	Inverted	Magnified
$s = f$		$\pm \infty$		
$s < f$	Virtual	$-\infty < p < 0$	Erect	Magnified

Based on the basic properties of a single lens, systems comprising multiple lenses can be conveniently designed. The resolution of an optical system is however beyond the scope of ray optics and has to be examined by wave optics. Owing to the diffractive nature of light, the best resolution of a lens system is limited to about half of the working wavelength  $\sim \lambda/2$  [3]. Using the immersion technique, the resolution can be improved up to  $\sim \lambda/(2n)$ , but such enhancement however is quite modest due to the low refractive index  $n$  of natural materials [4, 5]. To achieve higher resolution, a material that can support the propagation of light with higher  $k$ -vectors is needed. Metamaterials, which are artificially engineered nanocomposites possessing extraordinary material properties, provide new opportunities for this purpose [6–

8]. Various metamaterial based lenses have been proposed and demonstrated within the last decade [9–21]. Despite their success in achieving super resolution, such superlenses behave distinctively to their conventional counterpart. For instance, they cannot focus a plane wave, which represents a significant defect from both theoretical and practical points of view.

## 2. Theory

By introducing various phase compensation mechanisms in metamaterials, the plane wave focusing function has been realized recently [22, 23]. In this paper, we first provide a generalized imaging equation for the phase compensated metamaterials lenses, in which focal lengths can be defined from either direction. We further illustrate the unprecedented imaging properties if such lenses also experience negative refraction at the lens/air interfaces.

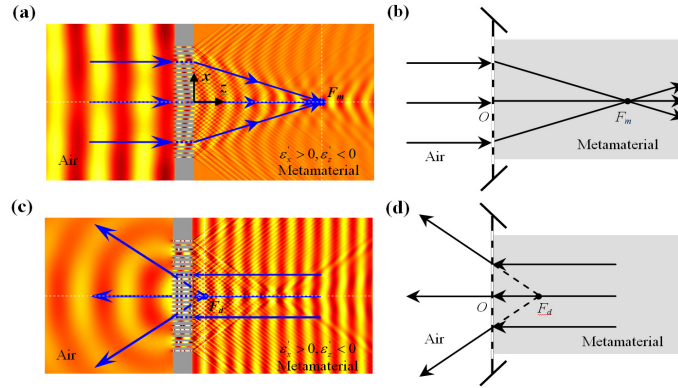


Fig. 2. Focusing behaviors of a hyperbolic metalens. (a) Plane wave from air converges to a focus ( $F_m$ ) in metamaterial. (c) Plane wave from metamaterial diverges in air, resulting in a virtual focus ( $F_d$ ) also in metamaterial. The arrows in (a) and (c) are eye-guiding rays. (b) and (d) Symbolized representation of (a) and (c). The dashed vertical lines represent phase compensating elements at the interfaces, i.e. the PWC.

By convenience, we use the hyperbolic metalens, which comprises a metal plasmonic waveguide coupler (PWC) (gray structure in Fig. 2(a) and 2(c)) and plasmonic metamaterials with hyperbolic dispersion ( $\epsilon_x' > 0$ ,  $\epsilon_z' < 0$ ), as a specific example to illustrate the new imaging paradigm. Such a hyperbolic metalens can be designed to focus an incident  $p$ -polarized plane wave from the air side to the focus  $F_m$  at the focal length  $f_m$  in the metamaterial by given  $\epsilon_x'$  and  $\epsilon_z'$ . The details of the PWC design follows similar principles described in literatures [23–25]. Due to the hyperbolic dispersion of the metalens, a plane wave comes from the metamaterial side, instead of being focused, diverges after the metalens, resulting in a virtual focus at  $F_d$  also in the metamaterial (Fig. 2(c)). It is well known that a conventional converging lens has two foci: one on each side; i.e., a plane wave coming from one side focuses to the other, and vice versa. In stark contrast, a hyperbolic metalens works like a converging lens from one side but a diverging lens from the other. Similar to a recent “Janus device” [26] showing different functions along multiple directions based on transformation optics [27, 28], a hyperbolic metalens is a “Janus lens” having two different focusing behaviors in opposite directions. Interestingly, although both focal lengths can be clearly defined, different signs must be taken accordingly. This distinctive focusing behavior leads to extraordinary imaging properties that do not exist in common lenses.

## 3. Formulations and simulations

An image  $P_d$  in air is formed by an object  $P_m$  in the metamaterial, and vice versa, as schematically shown in Fig. 3(a). The optical path length (OPL) from  $P_d$  to  $P_m$  is given by  $(\phi_d + \phi_m + \phi_c) / k_0$ , where  $\phi_d = k_0 \sqrt{v_d^2 + x^2}$  is the phase delay in air,  $\phi_m = k_0 \sqrt{\epsilon_x' v_m^2 + \epsilon_z' x^2}$  is

the phase delay in the metamaterial, and  $\phi_c = \phi_{const} - k_0 \sqrt{\epsilon_x' f_m^2 + \epsilon_z' x^2}$  is the designed phase delay profile of the PWC according to the metalens design principle.  $\epsilon_x'$  and  $\epsilon_z'$  are the real part of the metamaterial permittivity in  $x$  and  $z$  directions respectively.  $v_d$  and  $v_m$  are the image/object distances in air and metamaterial, and  $\phi_{const}$  is a constant.

According to the Fermat's Principle, the *OPL* remains stationary; that is, its derivative with respect to the position variable  $x$  is zero, i.e.,  $d[OPL]/dx = 0$ . So we have

$$\frac{1}{\sqrt{v_d^2 + x^2}} + \frac{\epsilon_z'}{\sqrt{\epsilon_x' v_m^2 + \epsilon_z' x^2}} = \frac{\epsilon_z'}{\sqrt{\epsilon_x' f_m^2 + \epsilon_z' x^2}} \quad (1)$$

This relationship must hold true for all the rays from  $P_m$  to  $P_d$ . Considering the paraxial approximation ( $x$  is negligible), Eq. (1) can be reduced to

$$\frac{1}{v_d} + \frac{\epsilon_z' / \sqrt{\epsilon_x'}}{v_m} = \frac{\epsilon_z' / \sqrt{\epsilon_x'}}{f_m} \quad (2)$$

It can be seen from Eq. (2) that when  $v_m \rightarrow \infty$ , i.e., the incident beam is a plane wave from the metamaterial, the focal length in air is resulted as  $f_d = f_m \sqrt{\epsilon_x' / \epsilon_z'}$ . Replacing  $f_d$  into Eq. (2), we obtain another form of metalens imaging equation

$$\frac{1}{v_d} + \frac{\epsilon_z' / \sqrt{\epsilon_x'}}{v_m} = \frac{1}{f_d} \quad (3)$$

Because of the hyperbolic dispersion of the metamaterial, the relation between  $f_d$  and  $f_m$  indicates they always have different signs. According to the sign convention, if  $f_m > 0$  represents  $F_m$  in the metamaterial (Fig. 2 (a)),  $f_d < 0$  means that the  $F_d$  is not in air but also in the metamaterial. Through an analogy to the typical symbolic notation of a focusing lens by using a double arrowed line, we symbolize the hyperbolic metalens with both foci in the metamaterial, as shown in Fig. 2(b) and 2(d).

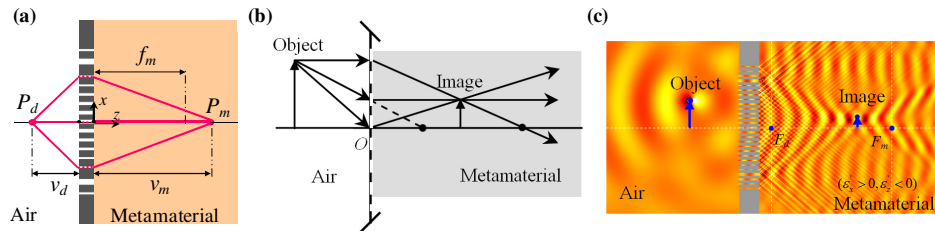


Fig. 3. (a) Schematic representation of forming an image by a hyperbolic metalens. Imaging behavior of a hyperbolic metalens for an object in air: (b) Ray diagram, (c) Numerical result.

As is analyzed above, a hyperbolic metalens breaks the forward/backward symmetry preserved in conventional lenses, leading to exceptional focusing behaviors. In the following, we examine the imaging formation for an object placed at various locations with respect to its focal lengths. The specific hyperbolic metalens was designed with  $f_m = 2.0 \mu\text{m}$  at the wavelength of 690 nm. The metamaterial is assumed to have  $\epsilon_x = 6.4 + 0.03i$  and  $\epsilon_z = -10.3 + 0.2i$ . This specific metamaterial can be constructed by silver nanowires in a dielectric host with a refractive index of 1.3. The silver nanowires are orientated in the  $z$  direction and their volumetric filling ratio is 0.5.

Figure 3(a) schematically depicts the imaging behavior of such a hyperbolic metalens for an object in air. Two characteristic rays can be used to determine the image: the one parallel to the optical axis is “refracted” toward the focus  $F_m$  in the metamaterial; another one towards the focus  $F_d$  is “refracted” to the direction parallel to the optical axis in the metamaterial. The

crossing point of these two rays determines the location of the image. Particularly, in the case of an object in air, the image in the metamaterial is always minified, erect, real and within the first focal length, regardless of the distance of the object in air to the metalens. This is completely different from a conventional lens, in which the image properties are dependent on the position of the object (see Table 1). Another special ray, which is the one passing the optical center  $O$ , may also be used to determine the location of the image through the calculation of its refraction angle in the metamaterial  $\theta_m \approx \text{Re}(\sqrt{\epsilon_x} / \epsilon_z) \sin \theta_d$ , with  $\theta_d$  being the incident angle and  $\theta_m$  being the refracted angle of that ray with respect to the optical axis. Figure 3(b) shows the numerical verification for such a case using full wave simulation. Because the image cannot go beyond the focal plane in the metamaterial, the entire half space in air is mapped into a highly confined region in metamaterial.

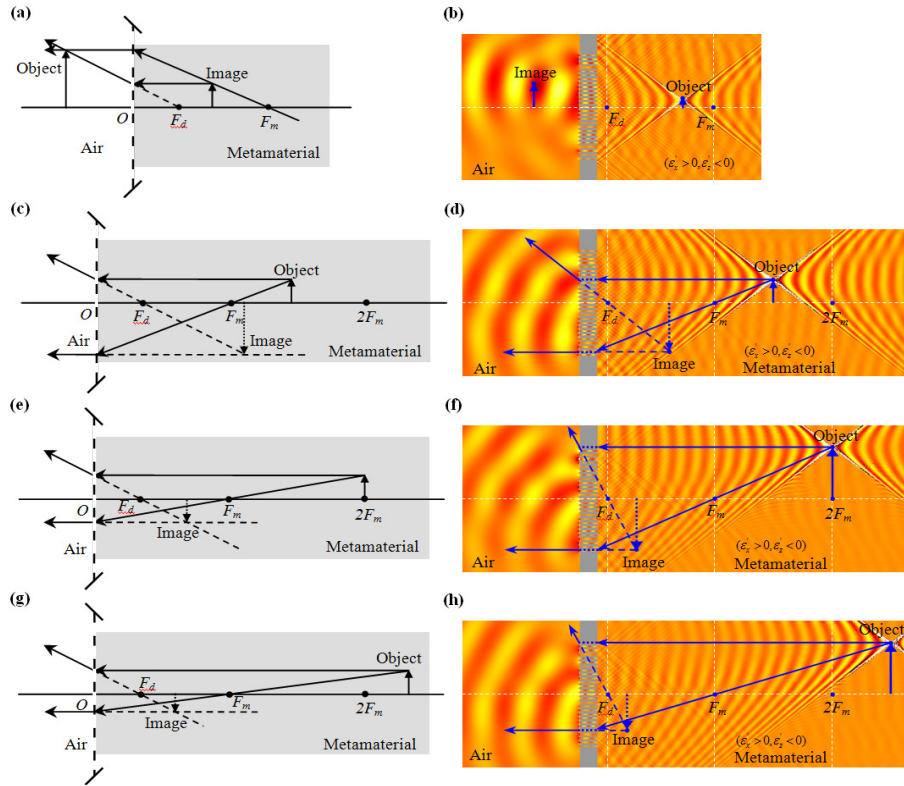


Fig. 4. Imaging behavior of a hyperbolic metalens for an object in metamaterial. (a) Object is inside point  $F_m$ . (c) Object is between points  $F_m$  and  $2F_m$ . (e) Object is at point  $2F_m$ . (g) Object is outside point  $2F_m$ . (b), (d), (f), (h), Numerical verifications of (a), (c), (e), (g), respectively.

Similarly, through schematic and geometric analysis, the image of an object in metamaterial can also be analyzed: the property of the image is dependent on the position of the object relative to the focus  $f_m$ . The image location can also be determined using characteristic rays: the one connecting the object and the focus  $F_m$  is “refracted” to the direction parallel to the optical axis; another one parallel to the optical axis is “refracted” to the direction whose backward extension passes the focus  $F_d$ , because  $F_d$  is not in air but in the metamaterial. Figure 4(a) shows the imaging behavior of an object within the first focal length in the metamaterial, i.e.,  $v_m < f_m$ : the image in air is always magnified, erect and real. The image is real because the “refracted” rays converge in air. This case is simply the reciprocal of the case shown in Fig. 3(b). When the object is outside the first focal length, i.e.,  $v_m > f_m$  the rays in air diverge, but their backward extensions converge into a point on the other side of

the optical axis in the metamaterial space, thus the image is always virtual and inverted. Depending on the relative position of the object, the image may be different in size; when the object is outside the first but inside the second focal length, i.e.,  $f_m < v_m < 2f_m$ , the image is magnified, as shown in Fig. 4(c); when the object is at the second focal length, i.e.,  $v_m = 2f_m$ , the image has the same size as the object, as shown in Fig. 4(e); when the object is outside the second focal length, i.e.,  $v_m > 2f_m$ , the image is minified, as shown in Fig. 4(g). All the four cases above for an object in the metamaterial are numerically verified, as shown in Fig. 4(b)-(h). These extraordinary properties of a hyperbolic metalens are summarized in Table 2, which can also be directly derived from the metalens imaging equations (Eq. (2) and (3)).

**Table 2. Imaging Properties of a Hyperbolic Metalens.  $f_m > 0$  and  $f_d < 0$ .**

Object	Image			
	Type	Location	Orientation	Relative size
$\infty > v_d > 0$	Real	$0 < v_m < f_m$	Erect	Minified
$\infty > v_m > 2f_m$	Virtual	$2f_d < v_d < f_d$	Inverted	Minified
$v_m = 2f_m$	Virtual	$v_d = 2f_d$	Inverted	Same size
$f_m < v_m < 2f_m$	Virtual	$-\infty < v_d < 2f_d$	Inverted	Magnified
$v_m = f_m$		$\pm \infty$		
$v_m < f_m$	Real	$0 < v_d < \infty$	Erect	Magnified

As shown in Fig. 3 and Fig. 4, the magnification of the metalens can also be determined analytically through the transverse magnification  $M_T$

$$M_T = \frac{u_m}{u_d} = -\frac{g_m}{f_m} = -\frac{f_d}{g_d} \quad (4)$$

where  $u_m$  and  $u_d$  are the object/image height, i.e., the distance from the object/image to the optical axis, in the metamaterial and air space respectively;  $g_m$  and  $g_d$  are the object/image distance reckoned from their focus in the metamaterial and air space respectively.

#### 4. Discussions and conclusions

Although illustrated using hyperbolic metalenses with  $f_m > 0$ ,  $f_m$  can also be designed to be negative ( $f_m < 0$ ), meaning a plane wave from the air side diverges in the hyperbolically dispersive metamaterial. In this case, a plane wave from the metamaterial side will be focused in air, resulting in a positive  $f_d$ . Analyses show that all the above equations remain valid and the hyperbolic metalens with  $f_m < 0$  is also a ‘‘Janus lens’’. The imaging properties of such a hyperbolic metalens with  $f_m < 0$  can also be deduced through a similar method mentioned above.

We finally emphasize that the new set of imaging properties in the exemplified hyperbolic metalens is a result of the hyperbolic dispersion of the metamaterials. The hyperbolic metalenses also possess super resolution capabilities as demonstrated before [23, 24]. The rules are applicable to any other type of phase compensated lenses that experiences negative refraction at the air/lens interface. These exotic imaging properties are impossible to realize by conventional lenses, thus extending the imaging properties and the capabilities of lenses, and the imaging optics in general, to a new horizon. A practical usage of such lenses is to truncate the metamaterial to the focal/image plane so that the optical near field can be accessed from air [29]. The new found imaging behaviors and the super resolving power of hyperbolic metalenses provide new opportunities to explore novel optical devices and systems and will profoundly affect the advancement of optics.

#### Acknowledgment

This work was partially supported by the startup fund of the University of California at San Diego and the NSF-ECCS under Grant No. 0969405.